

# UC Berkeley

## UC Berkeley Previously Published Works

### Title

Population toxicokinetics of benzene.

### Permalink

<https://escholarship.org/uc/item/14g0d92b>

### Journal

Environmental Health Perspectives, 104(Suppl 6)

### ISSN

1542-4359

### Authors

Bois, FY  
Jackson, ET  
Pekari, K  
et al.

### Publication Date

1996-12-01

### DOI

10.1289/ehp.961041405

Peer reviewed

# Population Toxicokinetics of Benzene

Frédéric Yves Bois,<sup>1</sup> Elise T. Jackson,<sup>1</sup> Kaija Pekari,<sup>2</sup> and Martyn T. Smith<sup>1</sup>

<sup>1</sup>Division of Environmental Health Sciences, School of Public Health, University of California, Berkeley, California; <sup>2</sup>Institute of Occupational Health, Helsinki, Finland

In assessing the distribution and metabolism of toxic compounds in the body, measurements are not always feasible for ethical or technical reasons. Computer modeling offers a reasonable alternative, but the variability and complexity of biological systems pose unique challenges in model building and adjustment. Recent tools from population pharmacokinetics, Bayesian statistical inference, and physiological modeling can be brought together to solve these problems. As an example, we modeled the distribution and metabolism of benzene in humans. We derive statistical distributions for the parameters of a physiological model of benzene, on the basis of existing data. The model adequately fits both prior physiological information and experimental data. An estimate of the relationship between benzene exposure (up to 10 ppm) and fraction metabolized in the bone marrow is obtained and is shown to be linear for the subjects studied. Our median population estimate for the fraction of benzene metabolized, independent of exposure levels, is 52% (90% confidence interval, 47–67%). At levels approaching occupational inhalation exposure (continuous 1 ppm exposure), the estimated quantity metabolized in the bone marrow ranges from 2 to 40 mg/day. — Environ Health Perspect 104(Suppl 6):1405–1411 (1996)

Key words: benzene, Gibbs sampling, human exposure, metabolism, toxicokinetics

## Introduction

Benzene is carcinogenic in animals and humans via one or several of its metabolites (1). Thus, the fraction metabolized is likely to be a better measure of toxic exposure than benzene exposure itself. However, the extent of benzene intake metabolized at low exposure levels in humans is still unknown. For humans this fraction is difficult to measure directly, but can be estimated with a physiological toxicokinetic model (2–5). These compartmental models (Figure 1) allow the simulation of a variety of end points in specific organs, while providing the opportunity to use relevant prior information on physiological parameters, such as blood flows, organ volumes, etc. (6).

Many of the model parameters, typically those controlling metabolism, are not known with precision. Proper statistical inference about the value of these parameters is therefore necessary, while conserving the strong prior information conferred by their physiological definition. Bayesian statistics also provide a natural way to merge *a priori* knowledge, gained by implementing a physiological model, with the experimental data. In addition, our interests reside in inference about benzene metabolism in humans, i.e., in a diverse population, rather than in any one individual studied in published experiments. We therefore designed a statistical model describing the relationships between individual and population physiological parameters to estimate population variability (7–10). Linking a statistical model to a physiological mechanistic model may seem a daunting task, given the number of parameters involved. In fact, up to now, little consideration has been given to statistical issues when using such models (11); however, for such difficult problems, Bayesian numerical methods can provide solutions (10). We describe the application to our model of Markov-chain Monte Carlo simulation, which is a simple and powerful tool. As a result we report predictions and confidence bounds on various

measures of benzene metabolism in a human population. We discuss how this information can improve our understanding of benzene toxicology.

## Methods

### Data and Models

The data consisted of the concentrations of benzene in exhaled air and venous blood, and phenol in urine, for three male volunteers exposed to benzene in an inhalation chamber during 4 hr (12). Data were collected during exposure and over the following 2 days. Two exposure levels were used: 1.7 ppm (5.2 µg/liter) and 10 ppm (30 µg/liter). Phenol concentrations were recorded only at the 10 ppm exposure level and were corrected for urine density. Two unreliable phenol measurements were discarded from this analysis (the corresponding urine density was low and density correction would not apply well). The small (barely detectable) contamination of the subjects' exhaled air prior to the 1.7-ppm exposure was ignored. This contamination cannot be a carryover from the previous 10-ppm exposure because 1 month separated the two experiments. In addition, the body weight of each individual was recorded (55, 73, and 90 kg, for subjects 1, 2, and 3, respectively), as well the minute volume for subject 2 (11 liters/min ± 10%).

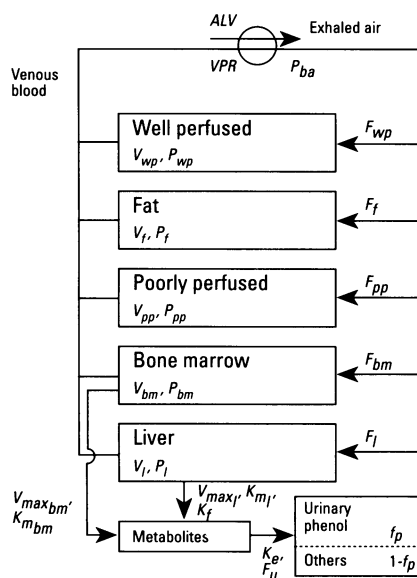


**Figure 1.** Schematic representation of the five-compartment physiological model used to simulate the distribution and metabolism of benzene.

This paper was presented at Benzene '95: An International Conference on the Toxicity, Carcinogenesis, and Epidemiology of Benzene held 17–20 June 1995 in Piscataway, New Jersey. Manuscript received 16 January 1996; manuscript accepted 14 June 1996.

The work of M.T. Smith and E. Jackson has been supported by a contract from Cal/EPA. The experimental work carried on in the Finnish Institute of Occupational Health was supported by the Finnish Work Environment Fund. Dr. Bois is in part supported by a grant from the Fondation de France.

Address correspondence to Dr. F.Y. Bois, B3E, INSERM U263, Room 307, 27 rue Chaligny, 75012 Paris, France. Telephone: (33) 1 44 73 84 44. Fax: (33) 1 44 73 84 62. E-mail: fbois@diana.lbl.gov

We used a physiologically based pharmacokinetic (PBPK) model in which the human body is divided into five compartments: poorly perfused tissues, well-perfused tissues, fat, bone marrow, and liver (Figure 1). These compartments are assumed to be homogeneous and distribution limited by blood flow. Pulmonary exchanges are modeled by assuming instantaneous equilibrium between alveolar air, venous blood, and arterial blood. Differential equations of the form

$$\frac{\partial C_i}{\partial t} = \frac{F_i}{V_i} \left( C_{art} - \frac{C_i}{P_i} \right)$$

describe the time dependence of the concentration  $C_i$  of benzene in each

compartment  $i$  as a function of blood flow,  $F_i$ , volume,  $V_i$ , arterial blood concentration,  $C_{art}$ , and partition coefficient,  $P_i$ . These equations are linear, except for the bone marrow and liver compartments, in which a Michaelis-Menten term describes the metabolic clearance of benzene. For these compartments:

$$\frac{\partial C_i}{\partial t} = \frac{F_i}{V_i} \left( C_{art} - \frac{C_i}{P_i} \right) - \frac{V_{max_i} C_i}{K_{m_i} + C_i V_i}$$

where  $V_{max_i}$  is the maximum rate of metabolism and  $K_{m_i}$  the Michaelis-Menten coefficient. The model also describes the endogenous formation of phenolic metabolites in the liver (at a constant rate,  $K_f$ ). These metabolites are supposed to be

eliminated from the liver and bone marrow to urine by a first-order process (with constant  $K_f$ ). Phenol itself represents a fraction,  $f_p$ , of the urinary metabolites. Computing the concentration of phenol in urine requires defining the urine formation rate,  $F_u$ . A list of the parameters is given in Table 1. The differentials were solved numerically using our own software, MCSim. The model allows us to compute, for given parameter values and initial exposure conditions, various quantities relevant for our purpose: concentration of benzene in blood or exhaled air, concentration of phenol in urine (during baseline conditions and benzene exposure), and quantity of benzene metabolized in a given period of time in the liver or bone marrow.

The statistical model describing uncertainties and variabilities was constructed using a hierarchical population approach (9,13), as illustrated in Figure 2. It has two major components: the individual level and the population level. At the individual's level, for each of three subjects, exhaled air and blood benzene concentrations or urinary phenol concentrations ( $y$ ) were measured experimentally. The expected values of these concentrations are a function ( $f$ ) of exposure level ( $E$ ), time ( $t$ ), a set of physiological parameters of unknown values ( $\theta$ ), and a set of measured, covariate parameters ( $\phi$ ).  $E$ ,  $t$ ,  $\theta$ , and  $\phi$  are subject specific. The function  $f$  is the nonlinear

**Table 1.** Prior distributions of the population means and standard deviations for the scaling coefficients of benzene model parameters in humans.<sup>a</sup>

Scaled parameter	Scaling function <sup>b</sup>	Prior on $\mu$			Truncation
		exp(M)	exp(S)	exp( $\Sigma_0$ )	
Body weight (bw) <sup>c</sup>	—	73	—	1.5	20–250
Ventilation over perfusion ratio (VPR)	—	1.6	1.3	1.3	0.73–3.5
Blood flows per unit mass					
Well-perfused tissues ( $F_{wp}$ )	SC $\times$ $V_{wp}$	0.3	1.1	1.1	0.225–0.4
Poorly perfused tissues ( $F_{pp}$ )	SC $\times$ $V_{pp}$	0.046	1.1	1.1	0.035–0.06
Fat ( $F_f$ ) <sup>d</sup>	SC $\times$ $V_f \times 0.92$	0.028	1.1	1.1	0.02–0.037
Bone marrow ( $F_{bm}$ )	SC $\times$ $V_{bm}$	0.19	1.1	1.1	0.14–0.25
Liver ( $F_l$ )	SC $\times$ $V_l$	1	1.1	1.1	0.75–1.33
Volumes					
Well-perfused tissues ( $V_{wp}$ )	SC $\times$ LM	0.2	1.1	1.1	0.15–0.26
Poorly perfused tissues ( $V_{pp}$ ) <sup>e</sup>	—	—	—	—	—
Fat ( $V_f$ ) <sup>d</sup>	SC $\times$ bw/0.92	0.17	1.5	1.5	0.05–0.58
Bone marrow ( $V_{bm}$ )	SC $\times$ LM	0.05	1.1	1.1	0.038–0.067
Liver ( $V_l$ )	SC $\times$ LM	0.03	1.1	1.1	0.023–0.04
Blood/air partition coefficient ( $P_{ba}$ )	—	15	1.5	1.3	4.4–50
Tissue/blood partition coefficients					
Well-perfused tissues ( $P_{wp}$ )	—	1.5	1.5	1.3	0.45–5
Poorly perfused tissues ( $P_{pp}$ )	—	1.5	1.5	1.3	0.45–5
Fat ( $P_f$ )	—	30	1.5	1.3	9–100
Bone marrow ( $P_{bm}$ )	—	5	1.5	1.3	1.5–17
Liver ( $P_l$ )	—	1.5	1.5	1.3	0.45–5
Maximal rates of metabolism					
Liver ( $V_{max_l}$ )	SC $\times$ LM 0.7	0.1	5	2	0.0008–12.5
Bone marrow ( $V_{max_{bm}}$ )	SC $\times$ $V_{max_l}$	0.08	2	2	0.02–0.3
Michaelis-Menten coefficients					
Liver ( $K_{m_l}$ )	$V_{max_l}/SC$	0.05	5	2	0.0004–6.25
Bone marrow ( $K_{m_{bm}}$ )	$V_{max_{bm}}/SC$	0.05	5	2	0.0004–6.25
Endogenous metabolites formation rate ( $K_f$ )	—	0.007	2	1.5	0.00087–0.056
Metabolites excretion rate constant ( $K_e$ )	—	0.003	2	1.5	0.00037–0.024
Urine formation rate ( $F_u$ )	—	0.001	1.5	1.5	0.0003–0.0034
Phenol fraction of excreted metabolites ( $f_p$ )	—	0.8	1.1	1.3	0.6–1

<sup>a</sup>For all parameters the scaling coefficients are assumed to be lognormally distributed. <sup>b</sup>Scaled parameter =  $f(SC)$  where SC is the scaling coefficient (no scaling function means that no scaling is made). Units: weights in kg, flow in liters/min, volumes in liters,  $V_{max}$  in mg benzene/min,  $K_m$  in mg benzene,  $K_f$  in mg benzene/min,  $K_e$  in  $\text{min}^{-1}$ ,  $F_u$  in liters/min. LM is the lean body mass (body mass–fat mass). <sup>c</sup>The body weights from Pekari et al. were used (12). The distribution given was used for the population extrapolations. <sup>d</sup>The density of fat tissues is assumed to be 0.92. <sup>e</sup>This parameter was set at each Monte Carlo iteration so that the sum of the organ masses (plus skeleton, 17% of LM) matched the imposed or sampled body weight.

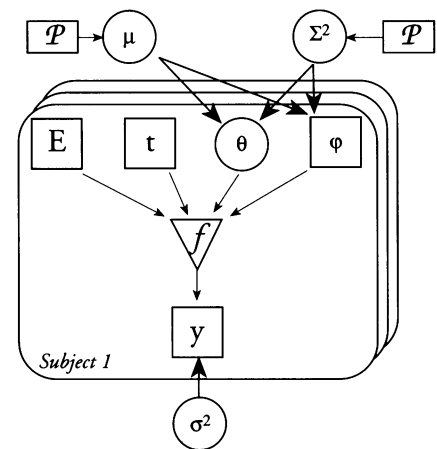


**Figure 2.** Graph of the statistical model describing the dependence relationships between several groups of variables.  $\mathcal{P}$ , prior distributions;  $\mu$ , mean population parameters;  $\Sigma^2$ , variances of the parameters in the population;  $E$ , benzene exposure concentrations;  $t$ , experimental sampling times;  $\theta$ , unknown physiological parameters;  $\phi$ , measured physiological parameters;  $f$ , toxicokinetic model;  $y$ , measured benzene concentrations in blood or exhaled air;  $\sigma^2$ , variance of the experimental measurements.

physiological model, described above. The concentrations actually observed are also affected by measurement errors, which are assumed, as usual, to be independent and log-normally distributed, with a mean of zero and a variance  $\sigma^2$  (on the log scale). The variance vector  $\sigma^2$  has three components,  $\sigma_1^2$  for the measurements in blood,  $\sigma_2^2$  for those in exhaled air, and  $\sigma_3^2$  for those in urine, because these measurements have different experimental protocols and therefore are likely to have different precisions. Given its relatively large imprecision, the minute volume for subject 2 was considered as a data point, with a fixed variance on the log scale (the value chosen corresponds to a 10% coefficient of variation ([CV]) in natural space).

Three types of nodes are featured in Figure 2: *a*) square nodes represent variables for which the values are known by observation, such as  $y$  or  $\phi$ ; were fixed by the experimenters, such as  $E$  and  $t$ ; or were fixed by ourselves, such as the prior on  $\mu$  and  $\Sigma^2$ ; *b*) circle nodes represent unknown variables, such as  $\theta$ ,  $\sigma^2$ ,  $\mu$ , or  $\Sigma^2$ ; *c*) following the notation of Thomas et al. (14), the triangle represents the deterministic physiological model  $f$ . An arrow between two nodes indicates a direct statistical dependence between the variables of those nodes.

### A Priori Parameter Distributions

To take into account known physiological dependencies between the toxicokinetic model parameters (e.g., between organ volumes and body weight, or alveolar ventilation rate and cardiac output) several of them were linked to the lean body mass or other parameter values via scaling functions (15–18) (Table 1). For example, volumes are input as fractions of the lean body weight, and the maximum rate of metabolism in liver as a power function of lean body weight. Note that cardiac output is computed as the sum of the organ flows. The scaling coefficients were the actual parameters used in input.

At the population's level, we assumed that each component of the  $\theta$  parameter set is distributed log-normally, with population averages  $\mu$  and variances  $\Sigma^2$  (in log scale). We have some *a priori* knowledge of  $\mu$  and  $\Sigma^2$ , at least in the form of standard values. We assigned *a priori* truncated normal distributions (with parameters  $M$  and  $S$  in log scale) to the population means  $\mu$ , and inverse gamma distributions (with parameter  $\Sigma_0^2$ ) for the population variances  $\Sigma_0^2$ . We defined prior value for the hyperparameters  $M$ ,  $S$ , and  $\Sigma_0^2$  on the basis of the

literature. The choice of values for these parameters and the bounds for truncation are summarized in Table 1. Truncations correspond for most parameters to 3 SDs to be subtracted or added to the mean. They are all biologically plausible. The exceptions are the two fractions  $V_{maxbm}$  and  $f_p$ , for which such truncation would be meaningless, and the body weight. In setting uncertainties (but not for variabilities), we tried to be conservative and set the prior variances higher rather than lower when there was ambiguity in the biological literature (for example, with the metabolic parameters). This weights down the prior variances to "let the data speak." For convenience we give in Table 1 the value of  $\exp(M)$  (i.e., the geometric mean of the scaling coefficients)  $\exp(S)$  and  $\exp(\Sigma_0)$ , which lie on the natural scale.

The values used for organ masses, when expressed as fractions of lean body weight, are usually considered as reference values for 35-year-old males (19,20). Volumes in liters and masses in kilograms have the same values since a density of 1.0 is assumed for all tissues, except for fat (density 0.92). Both the uncertainty on  $\mu$  and the heterogeneity of the fraction volumes in the population are estimated to be of the order of 10 to 15% (coefficient of variation), depending on the tissue group. As a consequence of scaling, the organ volumes are constrained by definition and have to sum to the lean body weight, not including bones, for each individual. We compute the volume of the poorly perfused compartment by difference so that the constraint is automatically satisfied at each iteration.

The geometric means of the perfusion rates per unit mass for the different compartments were set to usually accepted reference values (19,20). The mean ventilation over perfusion ratio (VPR) was set at 1.6 (21), since the subjects were allowed some activity after exposure.  $\exp(S)$  and  $\exp(\Sigma_0)$  were set at 1.1 for the flows to various tissues, and 1.3 for VPR. This corresponds approximately to 10 and 30% variability, respectively. Using perfusion rates accounts for the covariance between total organ perfusion and organ weight.

The geometric means used for benzene blood/air and tissue over blood partition coefficient are taken from ranges and values previously published (22–25). Partition coefficients may vary by a factor of 2 with hematocrit or depending on fasting, for example (26). Therefore,  $\exp(S)$  was set at 1.5 for all partition coefficients.  $\exp(\Sigma_0)$  was set to 1.3.

Prior estimates for the scaling coefficients for the population's maximum rates of metabolism in the liver and bone marrow,  $V_{maxl}$ ,  $V_{maxbm}$ , and for the ratios of the maximum rates to the Michaelis-Menten coefficients,  $K_{ml}$ ,  $K_{mbm}$ , were taken from the literature (22,23,25). A large uncertainty is still associated with these numbers, and we chose a value of 5 for  $\exp(S)$ , except for  $V_{maxbm}$ , which is the ratio of marrow to liver metabolism. We set  $\exp(\Sigma_0)$  at 2. Thus, we believe these parameters to vary in the population of Pekari et al. subjects by about a factor of 2, but we are uncertain by a factor of 5 as to their population means. It would be difficult to express this sort of uncertainty without an explicit hierarchical model.

Prior variance for the average urine flow,  $F_w$ , was set on the basis of Rowland and Tozer (27), with likely uncertainty and variability of about 50%. The fraction of phenol in the urinary metabolites,  $f_p$ , ranges from 0.6 to about 1 (25), and we set its geometric mean to 0.8, with  $\exp(S)$  at 1.1 and  $\exp(\Sigma_0)$  at 1.3. The excretory half-life of phenol,  $K_e$  is 4.5 hr (28), so we set the excretion rate to 0.003/min, with a large uncertainty and a 50% CV for variability. The average amount of phenol in urine of subjects unexposed to benzene is 6 mg/liter and ranges from about 1 mg/liter to 40 mg/liter (12): given that at equilibrium  $K_f = (\text{phenol concentration}) \times F_u/f_p$ , it can be deduced that the mean of  $K_f$  should be approximately 0.007 mg/min; we set uncertainty and variability to the plausible values used for  $K_e$ .

At the individual level, we had no prior information for most of the parameters (except for the measured covariates), so information about the distribution of an individual's  $\theta$  parameter values is given by the experimental data and by the population parameters,  $\mu$  and  $\Sigma^2$ .

### Statistical Computations

A Bayesian analysis allowed us to combine two forms of information: "prior knowledge" from the scientific literature, and "data" from Pekari's experiments, in the context of the physiological compartmental model. Neither source of information is complete. If prior knowledge were sufficient, the experiments would not have had to be done, but Pekari's data alone are insufficient to pin down the parameters to reasonable values. Our goal was to fit the data using scientifically plausible parameter values.

The second interesting feature of the Bayesian approach is that it produces a

posterior distribution for the parameters, rather than a mere point estimate. Thus, the analysis outputs distributions of parameter values that are consistent with both the data and the prior information. Our statistical analysis yields distributional estimates (posterior distributions) of the parameters for each subject and for the population.

Current standard practice in Bayesian statistics is to summarize a complicated high-dimensional posterior distribution by random draws of the vector of parameters, in this case, from the distribution  $P(\theta, \mu, \Sigma^2, \sigma^2 | \text{data prior})$ . The simulations can then be used to compute posterior distributions of estimands of interest, including individual parameters, and also derived quantities such as the proportion of benzene metabolized under specified conditions. Because  $\theta$  has many components, we use a combination of Gibbs sampling and Metropolis-Hasting Monte Carlo sampling to perform a random walk through the posterior distribution. These samplings are iterative procedures particularly convenient in the case of hierarchical models. They belong to a class of Markov-chain Monte Carlo techniques that has recently received much interest (8,10,29–31). Five independent Monte Carlo runs were performed. Convergence was monitored using the method of Gelman and Rubin (32).

### Population Extrapolation

The distributions of the fraction of benzene metabolized in the bone marrow or liver at various continuous exposure levels to benzene (0.001 ppm to 10 ppm) were obtained by simulation over 3 weeks. We verified that equilibrium was always reached in those conditions (the amounts metabolized over the last day differed at most by half a percent from the previous day). To compute the fraction metabolized over the last day, the amount metabolized was divided by the amount inhaled on the same day (i.e., the product of the alveolar ventilation volume for a day by the benzene inhalation level). These simulations were performed for the population by sampling one random parameter vector from  $N(\mu, \Sigma)$  for each of the 5000 estimates of  $\mu$  and  $\Sigma$ . This accounts for parameter covariance since the  $5 \times 1000$  individual and population parameter sets are random draws from their joint (multivariate) distribution, not just from the marginal distributions, as would be the case in simple Monte Carlo simulations. For these simulations, body mass was also sampled lognormally (with geometric mean and standard deviation given in Table 1) (20).

## Results and Discussion

### Model Fit

The use of the Markov chain simulations, which reached approximate convergence in about 20,000 iterations, has allowed us to obtain a very good fit to the data of Pekari et al., while maintaining scientifically plausible parameter values. Figure 3 shows the data values predicted for each individual versus their observed counterparts (all data values are concentrations). Predictions were made with the highest posterior parameter values. This iteration is not much better than any of the last 5000 and is quite representative of the set. For an optimal fit, all points would fall on the diagonal, but such an adjustment is not expected given the analytical measurement errors in the data. The deviations here are small and the fit seems reasonable. Figures 4 and 5 give the simulated time profiles for subject 1, together with the data points. The experimental SDs estimates are  $0.22 \pm 0.016$ ,  $0.17 \pm 0.013$ , and  $0.22 \pm 0.017$  (in log space) for the venous blood, exhaled air, and urinary

phenol measurements, respectively. These correspond approximately to CVs of 24, 19, and 24%. The data points are bracketed in the figures by 2 SDs to give an idea of their precision. Fits for the other subjects are similar in quality.

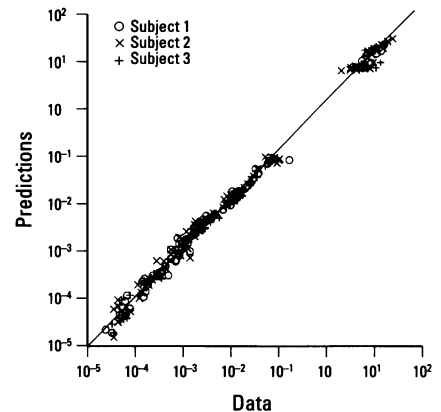


**Figure 3.** Predicted versus observed data values (blood and exhaled air benzene concentrations, and urinary phenol concentrations) for the best iteration of the last 5000 Markov-chain Monte Carlo runs.

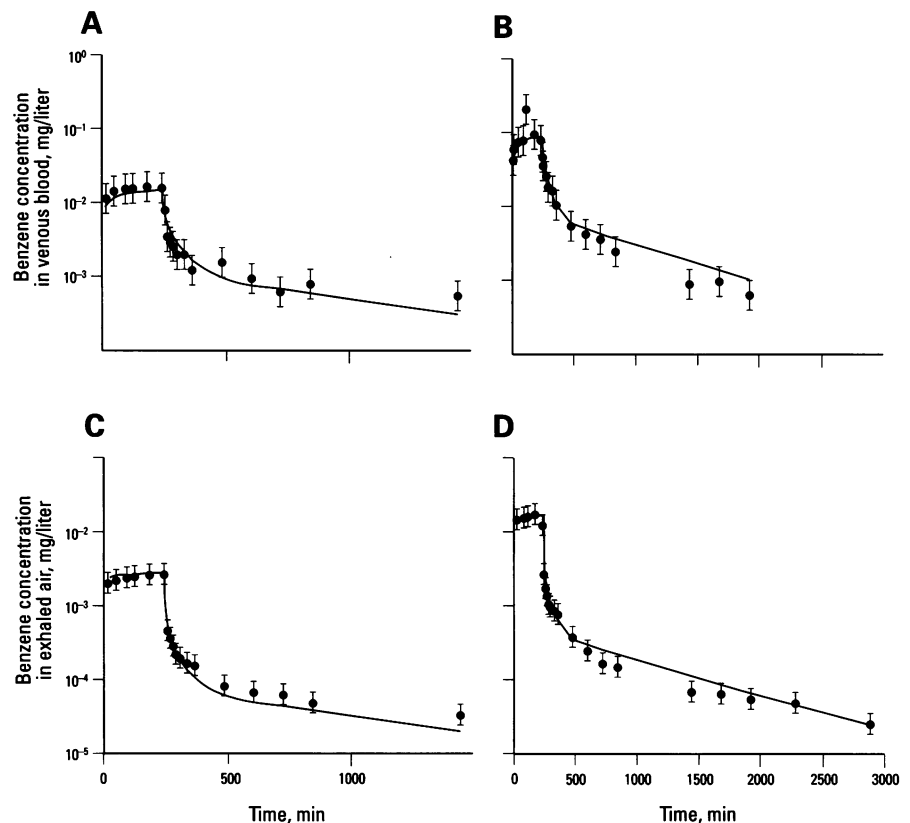


**Figure 4.** Simulated and observed time course of the venous blood and exhaled air concentrations of benzene in subject 1 [data of Pekari et al. (12)]. Exposures were to 10 ppm (A, C) and 1.7 ppm (B, D) for 4 hr. The data points are bracketed by  $\pm 2$  estimated SDs. Results are similar for the other two subjects.

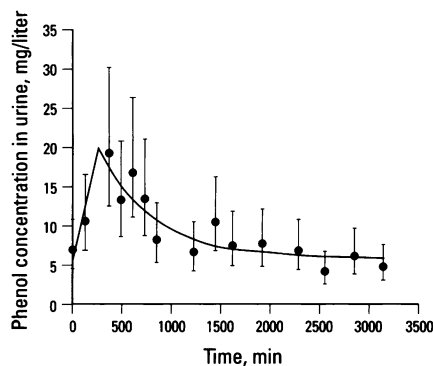


**Figure 5.** Simulated and observed time course of urinary phenol concentrations for subject 1 [data of Pekari et al. (12)]. Exposure was 10 ppm (30 µg/liter) for 4 hr, starting at time zero. The data points are bracketed by ± 2 estimated SDs. Results are similar for the other two subjects.

In its present form, the model accounts for uncertainty and intersubject variability but not for intrasubject variability. The second exposure was performed 1 month after the first, and subject variability is the most likely explanation for the slight under- or overestimations of the terminal slopes. A problem is that intrasubject variability confounds the dose effect. A better experimental design would have exposed the subjects

twice to each benzene concentration level. The parameter values found for each subject should therefore be considered as approximate averages for that individual.

**Posterior Distributions: Parameter Values**

Among the results are the posterior distributions of all parameter values for individuals (whose precision is affected by measurement errors) and for the population (whose precision depends on population heterogeneity). The posterior distributions of the individuals' and population's parameters are summarized in Table 2 (the last 1000 iterations of the five runs were pooled, and the distributions are established with 5000 values).

The location of many parameters is noticeably different from the corresponding prior mean. However, the posterior distributions for most parameters are consistent with their prior distributions. The most important shifts are observed for the volume of fat, the partition coefficients and the metabolic parameters. The partition coefficients are quite close to those found by Watanabe et al. (25). However, the values of the scaling coefficients for the metabolic parameters  $V_{max}$  and  $K_m$  in the liver and bone marrow are different from what has

been previously assumed or found. The mean of the scaling coefficient of the maximum rate of metabolism in the liver is about 60 times higher than the prior mean. The maximum rate in the bone marrow is expressed as a fraction, about 16%, of that in liver and therefore follows a similar trend. A tension between prior and data can even be noticed: the population mean for these parameters is lower than the individual values. This is because the prior constrains the population mean more than the individual values, which are more influenced by the data. The prior pulls down the estimated population average. The explanation of these findings is the following: as will be illustrated below, benzene metabolism is essentially linear in the dose range studied. The estimates of  $V_{max}$  and  $K_m$  are therefore driven up by the estimation process. Only the  $V_{max}/K_m$  scaling coefficients retain a meaning as they correspond to the first order rate of metabolism in the organs. The posterior mode (the point of highest probability) of the mean population  $V_{max}/K_m$  ratio for the liver is 0.6/min, with a population average of 0.76/min (Figure 6). For the bone marrow the mode is 2.8/min and the population average 1.12/min, which indicates that metabolism is significant in this organ.

**Table 2.** Summary of the posterior (fitted) distributions for the scaling coefficients of the model parameters.

Scaled parameter	Scaling coefficient value			Population geometric mean, exp(µ)	Population SD, exp(Σ) <sup>2</sup>
	Subject 1	Subject 2	Subject 3		
VPR	1.8 ± 0.23	1.6 ± 0.15	1.8 ± 0.25	1.7 ± 0.20	1.14 × ± 1.02
$F_{wp}$	0.35 ± 0.025	0.34 ± 0.025	0.34 ± 0.025	0.34 ± 0.022	1.05 × ± 1.01
$F_{pp}$	0.040 ± 0.0028	0.041 ± 0.003	0.040 ± 0.003	0.041 ± 0.0026	1.05 × ± 1.01
$F_f$	0.029 ± 0.0028	0.029 ± 0.0028	0.028 ± 0.003	0.029 ± 0.0024	1.05 × ± 1.01
$F_{bm}$	0.20 ± 0.018	0.19 ± 0.018	0.20 ± 0.018	0.19 ± 0.016	1.05 × ± 1.01
$F_l$	1.0 ± 0.10	1.0 ± 0.095	1.0 ± 0.095	1.0 ± 0.084	1.05 × ± 1.01
$V_{wp}$	0.23 ± 0.016	0.23 ± 0.017	0.23 ± 0.017	0.23 ± 0.015	1.05 × ± 1.01
$V_f$	0.27 ± 0.029	0.24 ± 0.028	0.27 ± 0.030	0.25 ± 0.035	1.21 × ± 1.02
$V_{bm}$	0.05 ± 0.005	0.052 ± 0.005	0.052 ± 0.005	0.052 ± 0.004	1.05 × ± 1.01
$V_l$	0.032 ± 0.003	0.031 ± 0.0029	0.031 ± 0.003	0.031 ± 0.0026	1.05 × ± 1.01
$P_{ba}$	9.1 ± 0.49	10 ± 0.55	9 ± 0.54	9.65 ± 0.77	1.14 × ± 1.01
$P_{wp}$	0.94 ± 0.18	1.0 ± 0.19	1.0 ± 0.19	1.0 ± 0.18	1.14 × ± 1.02
$P_{pp}$	1.7 ± 0.23	1.6 ± 0.19	1.7 ± 0.22	1.7 ± 0.20	1.14 × ± 1.01
$P_f$	19 ± 2.1	17 ± 2.1	21 ± 2.3	19 ± 2.3	1.14 × ± 1.02
$P_{bm}$	7.8 ± 2.7	7.8 ± 2.6	7.8 ± 2.6	7.67 ± 2.5	1.14 × ± 1.02
$P_l$	1.9 ± 0.72	1.8 ± 0.71	1.9 ± 0.71	1.8 ± 0.66	1.14 × ± 1.02
$V_{max_l}$	6.3 ± 2.8	6.3 ± 2.8	6.3 ± 2.8	5.8 ± 2.4	1.41 × ± 1.05
$V_{max_{bm}}$	0.17 ± 0.063	0.17 ± 0.063	0.17 ± 0.063	0.16 ± 0.054	1.41 × ± 1.04
$K_{ml}$	0.63 ± 0.38	0.59 ± 0.34	0.66 ± 0.40	0.60 ± 0.35	1.39 × ± 1.04
$K_{m_{bm}}$	3.1 ± 1.4	3.0 ± 1.4	3.1 ± 1.4	2.8 ± 1.2	1.41 × ± 1.05
$K_f$	0.015 ± 0.0029	0.011 ± 0.0023	0.018 ± 0.004	0.014 ± 0.0027	1.25 × ± 1.04
$K_e$	0.0018 ± 0.0004	0.0020 ± 0.0004	0.0011 ± 0.0004	0.0016 ± 0.0004	1.28 × ± 1.05
$F_u$	0.0026 ± 0.0004	0.0025 ± 0.0003	0.0029 ± 0.0003	0.0025 ± 0.0003	1.22 × ± 1.02
$f_p$	0.79 ± 0.084	0.79 ± 0.085	0.72 ± 0.073	0.78 ± 0.06	1.14 × ± 1.01

The means and SDs of the posterior distributions were established using the last 1000 iterations of the five runs performed. The transformation  $1 - \exp(-\Sigma)$  gives an approximate coefficient of variation.

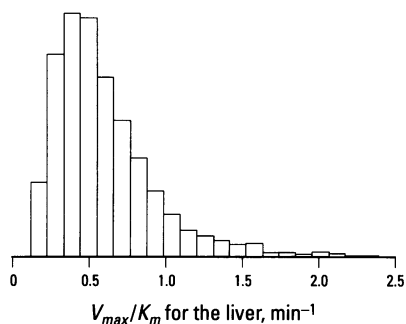


**Figure 6.** Estimated distribution of the mean rate constant of benzene metabolism in liver for a human population. The histogram is based on 5000 Markov-chain Monte Carlo runs, and represents uncertainty in the mean value.

However, a very large uncertainty affects this value: the bone marrow is a “hidden” compartment (from the point of view of the data at hand), and little information is available about its metabolism in humans. Uncertainty (summarized by the SDs given in Table 2), however, is largely reduced (by comparison to the prior S) for most of the other parameters, indicating that the data brought important information about them.

Interindividual variabilities are measured by the population standard deviations  $\Sigma$ , also given in Table 2. Those SDs correspond to factor 1.2 to 1.4 for the metabolic parameters. They are lower for the physiologic scaling coefficients. However, only three young white subjects were observed, and wider variations would certainly be found when observing a larger population. We noted above that it is likely that intra-subject variability affects the parameters (such as partition coefficients or metabolic parameters), but we did not attempt to estimate, as the data seemed insufficient for that purpose.

### Posterior Distributions: Fraction of Benzene Metabolized

The relationship between inhalation exposure level and fraction of benzene metabolized per unit time in the bone marrow, after 3 weeks of continuous exposure, is presented in Figure 7. A similar relationship

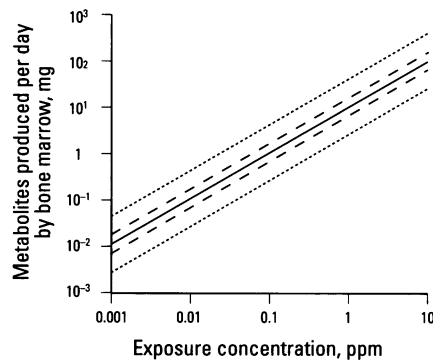


**Figure 7.** Simulated relationship between benzene exposure concentration and bone marrow metabolism in humans. The solid line gives the geometric mean population relationship; the dashed and dotted lines correspond to  $\pm 1$  and  $\pm 3$  population SDs, respectively (including uncertainty and variability). A linear relationship is also obtained for the liver.

is obtained in the liver. This relationship is linear over the data range and beyond. However, the curve above 10-ppm exposure levels is an extrapolation into a region in which saturation could occur, and interpretation should be careful in this respect. Watanabe et al. (25) found that saturation could occur beyond 100 ppm. They also found slight nonlinear effects (S-shaped curving) in the relationship, which we do not see here. The data of Pekari et al. is of far better quality than those used by Watanabe et al., and we put more confidence in the present results. However, nonlinearity may still be found in other populations or if more subjects were to be studied. Further, linearity in primary metabolism does not imply linearity in the subsequent enzymatic transformations of the metabolites. Recent work by McDonald et al. (33) also support the notion that benzene metabolism is linear at low levels: see also the review by Smith (34). It is reassuring that, regardless of slight differences in the shape of the relationship, the quantities of metabolites predicted by Watanabe et al. and by us are close (geometric mean 10 mg per day with SD corresponding to a factor 1.6, at 1 ppm exposure).

The population distribution of the total fraction metabolized is spread over a

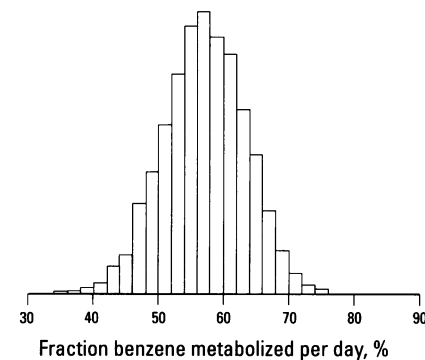


**Figure 8.** Estimated population distribution of the fraction of benzene metabolized by humans. This fraction is independent of the exposure level (at least up to 10 ppm exposure). The histogram is based on 5000 Markov-chain Monte Carlo runs and represents both uncertainty and variability.

relatively narrow range. At low exposure (0.001 ppm), the mean of 5000 Monte Carlo estimates of this fraction is 57% (SD 6%) and the 5th and 95th percentiles are 47 and 67%, respectively (Figure 8). The same results are obtained at high exposure (up to 10 ppm) because the relationship between amount metabolized and inhalation exposure is linear. It would be interesting to check what fraction of this variability can be explained by differences in P4502E1 activity, as measured, for example, by the chlorzoxazone assay (35,36).

These results are indeed conditioned by the use of a small data set, with only three subjects of similar characteristics. While uncertainty could be reduced by additional analyses, population variability, which in this study is approximately as large as uncertainty about individual subjects, could increase when more subjects are included. This type of analysis requires a population pharmacokinetic approach and is more sophisticated than simple Monte Carlo simulations for uncertainty assessment. The results of the population approach are far more reliable because they rely as heavily on human data as on *a priori* physiological information. The method is of general applicability and provides a basis for statistically valid inference with physiological models.

### REFERENCES

1. Snyder R, Kalf G. A perspective on benzene leukemogenesis. *Crit Rev Toxicol* 24:177–209 (1994).
2. Bois FY, Zeise L, Tozer TN. Precision and sensitivity analysis of pharmacokinetic models for cancer risk assessment: tetrachloroethylene in mice, rats and humans. *Toxicol Appl Pharmacol* 102:300–315 (1990).
3. Andersen ME, Krewski D, Withey JR. Physiological pharmacokinetics and cancer risk assessment. *Cancer Lett* 69:1–14 (1993).
4. Balant LP, Gex-Fabry M. Physiological pharmacokinetic modelling. *Xenobiotica* 20:1241–1257 (1990).

5. Gerlowski LE, Jain RK. Physiologically based pharmacokinetic modeling: principles and applications. *J Pharm Sci* 72:1103–1127 (1983).
6. Spear R, Bois F. Parameter variability and the interpretation of physiologically based pharmacokinetic modeling results. *Environ Health Perspect* 102 (Suppl 11):61–66 (1994).
7. Racine-Poon A, Smith AF. Population models. In: *Statistical Methodology in the Pharmaceutical Sciences* (Berry DA, ed). New York:Marcel Dekker, 1990;139–162.
8. Wakefield JC, Smith AFM, Racine-Poon A, Gelfand AE. Bayesian analysis of linear and non-linear population models using the Gibbs sampler. *Appl Stat - J Royal Stat Soc Series C* 43:201–221 (1994).
9. Wakefield JC. The Bayesian analysis of population pharmacokinetic models. *J Am Stat Soc* 91:62–75 (1995).
10. Bois FY, Gelman A, Jiang J, Maszle DR, Zeise L, Alexeef G. Population toxicokinetics of tetrachloroethylene. *Arch Toxicol* 70:347–355 (1996).
11. Woodruff TJ, Bois FY. Optimization issues in physiological toxicokinetic modeling—a case study with benzene. *Toxicol Lett* 69:181–196 (1993).
12. Pekari K, Vainioralo S, Heikkilä P, Palotie A, Luotamo M, Riihimäki V. Biological monitoring of occupational exposure to low levels of benzene. *Scand J Work Environ Health* 18:317–322 (1992).
13. Gelman A, Bois F, Jiang J. Physiological pharmacokinetic analysis using population modeling and informative prior distributions. *J Am Stat Assoc* (in press).
14. Thomas A, Spiegelhalter DJ, Gilks WR. BUGS: a program to perform Bayesian inference using Gibbs sampling. In: *Bayesian Statistics 4* (Bernardo JM, Berger JO, Dawid AP, Smith AFM, eds). Oxford:Oxford University Press, 1992;837–842.
15. Adolph EF. Quantitative relations in the physiological constitution of mammals. *Science* 109:579–585 (1949).
16. Davidson IWF, Parker JC, Beliles RP. Biological basis for extrapolation across mammalian species. *Regul Toxicol Pharmacol* 6:211–237 (1986).
17. Ings RM. Interspecies scaling and comparisons in drug development and toxicokinetics. *Xenobiotica* 20:1201–1231 (1990).
18. Mordenti J. Man versus beast: pharmacokinetic scaling in mammals. *J Pharm Sci* 75:1028–1040 (1986).
19. ICRP. Report of the Task Group on Reference Man—A Report Prepared by a Task Group of Committee 2 of the International Commission on Radiological Protection. Oxford: Pergamon Press, 1975.
20. Williams LR, Leggett RW. Reference values for resting blood flow to organs of man. *Clin Phys Physiol Meas* 10:187–217 (1989).
21. Astrand I. Effect of physical exercise on uptake, distribution and elimination of vapors in man. In: *Modeling of Inhalation Exposure to Vapors: Uptake, Distribution, and Elimination* (Fiserova-Bergerova F, ed). Boca Raton, FL:CRC Press, 1983;107–130.
22. Medinsky MA, Sabourin PJ, Lucier G, Birnbaum LS, Henderson RF. A physiological model for simulation of benzene metabolism by rats and mice. *Toxicol Appl Pharmacol* 99:193–206 (1989).
23. Travis CC, Quillen JL, Arms A. Pharmacokinetics of benzene. *Toxicol Appl Pharmacol* 102:400–420 (1990).
24. Bois FY, Woodruff TJ, Spear RC. Comparison of three physiologically-based pharmacokinetic models of benzene disposition. *Toxicol Appl Pharmacol* 110:79–88 (1991).
25. Watanabe K, Bois F, Daisey J, Auslander D, Spear R. Benzene toxicokinetics in humans—bone marrow exposure to metabolites. *Occup Environ Med* 51:414–420 (1994).
26. Fiserova-Bergerova V. Gases and their solubility: a review of fundamentals. In: *Modeling of Inhalation Exposure to Vapors: Uptake, Distribution, and Elimination* (Fiserova-Bergerova F, ed). Boca Raton, FL:CRC Press, 1983;3–28.
27. Rowland M, Tozer TN. *Clinical Pharmacokinetics: Concepts and Applications*, 2nd Ed. Philadelphia:Lea & Febiger, 1989.
28. Docter HJ, Zielhuis RL. Phenol excretion as a measure of benzene exposure. *Ann Occup Hyg* 10:317–326 (1967).
29. Gelfand AE, Smith AFM. Sampling-based approaches to calculating marginal densities. *J Am Stat Assoc* 85:398–409 (1990).
30. Gelman A. Iterative and non-iterative simulation algorithms. *Comput Sci Stat* 24:433–438 (1992).
31. Smith AFM. Bayesian computational methods. *Phil Transac Royal Soc London, Series A* 337:369–386 (1991).
32. Gelman A, Rubin DB. Inference from iterative simulation using multiple sequences (with discussion). *Stat Sci* 7:457–511 (1992).
33. McDonald T, Yeowell-O'Connell K, Rappaport S. Comparison of protein adducts of benzene oxide and benzoquinone in the blood and bone marrow of rats and mice exposed to [<sup>14</sup>C/<sup>13</sup>C6]benzene. *Cancer Res* 54:4907–4914 (1994).
34. Smith MT. Mechanistic studies of benzene toxicity: implications for assessment. In: *Biological Reactive Intermediates. 5: Basic Mechanistic Research in Toxicology and Human Risk Assessment* (Snyder R, Sipes GI, Kalf GF, eds). New York:Plenum Press, 1996;259–266.
35. Hoener B-A. Predicting the hepatic clearance of xenobiotics in humans from *in vitro* data. *Biopharm Drug Dispos* 15:295–304 (1994).
36. Seaton MJ, Schlosser PM, Bond JA, Medinsky MA. Benzene metabolism by human liver microsomes in relation to cytochrome P450 2E1 activity. *Carcinogenesis* 15:1799–1806 (1994).